International Journal of Engineering

Journal Homepage: www.ije.ir

Neuro-fuzzy Sliding Mode Controller Based on a Brushless Doubly Fed Induction Generator

L. Ouada*[a], S. Benaggoune[a], S. Belkacem[b]

[a] *Faculty of Technology, LSTE Laboratory, University of Mostefa Ben Boulaïd Batna 2, Algeria*
[b] *LEB Research Laboratory, Electrical Engineering Department, University of Mostefa Ben Boulaïd Batna 2, Algeria*

P A P E R I N F O

Paper history:
Received 30 June 2019
Received in revised form 07 January 2020
Accepted 16 January 2020

Keywords:
Brushless Doubly Fed Induction Generator
Neuro-fuzzy Sliding Mode Control
Parameters Uncertainly
Sliding Mode Control
Vector Control

A B S T R A C T

The combination of neural networks and fuzzy controllers is considered as the most efficient approach for different functions approximation, and indicates their ability to control nonlinear dynamical systems. This paper presents a hybrid control strategy called Neuro-Fuzzy Sliding Mode Control (NFSMC) based on the Brushless Doubly fed Induction Generator (BDFIG). This replaces the sliding surface of the control to exclude chattering phenomenon caused by the discontinuous control action. This technique offers attractive features, such as robustness to parameter variations. Simulations results of 2.5 KW BDFIG have been presented to validate the effectiveness and robustness of the proposed approach in the presence of uncertainties with respect to vector control (VC) and sliding mode control (SMC). We compare the static and dynamic characteristics of the three control techniques under the same operating conditions and in the same simulation configuration. The proposed controller schemes (NFSMC) are effective in reducing the ripple of active and reactive powers, effectively suppress sliding-mode chattering and the effects of parametric uncertainties not affecting system performance.

***doi**: 10.5829/ije.2020.33.02b.09*

NOMENCLATURE

V_{sp}, V_{sc}, V_r	Stator and rotor d-q reference frame voltages	R_r, R_{sc}, R_{sp}	Rotor; PW, PC resistances
I_{sp}, I_{sc}, I_r	Stator and rotor d-q reference frame currents	T_{em}	Electromagnetic torque
R_{sp}, R_{sc}, R_r	Stator winding resistances	**Abbreviations**	
L_r, L_{sp}, L_{sc}	Self-induction of PW and rotor winding	DFIG	Doubly Fed Induction Generator
L_{mp}	Mutual induction between PW and rotor	BDFIG	Brushless Doubly Fed Induction Generator
$\omega_c, \omega_p, \omega_n$	Stators synchronous angular frequency	NFSMC	Neuro-Fuzzy Sliding Mode Control
P_p, P_c	Pole pairs	SMC	Sliding Mode Control
L_{mc}	Mutual induction between CW and rotor	PI	Proportional Integral
P_c, Q_{sp}	Active and reactive powers	VC	Vector Control
$\psi_{sc}, \psi_{sp}, \psi_r$	Stator and rotor d-q reference frame fluxes	ANFIS	Adaptive Neural Fuzzy Inference System

1. INTRODUCTION

The renewable energy market has grown considerably in recent years. The intensive consumption of electrical energy and the increase in the price of hydrocarbons have led several countries to initiate national and international programs intended to produce electrical energy from renewable resources [1].

The double Fed induction generator (DFIG), the most useful model for the use of wind energy, is undeniable. However, because of the presence of a slip ring and

*Corresponding Author Email: *ouada.laid@gmail.com* (L. Ouada)

Please cite this article as: L. Ouada, S. Benaggoune, S. Belkacem, Neuro-fuzzy Sliding Mode Controller Based on a Brushless Doubly Fed Induction Generator, International Journal of Engineering (IJE), IJE TRANSACTIONS B: Applications Vol. 33, No. 2, (February 2020) 248-256

brushes that require more control and maintenance; its application in hostile environments is limited [2]. Thus, the emergence of Brushless Doubly fed Induction Generator (BDFIG) has made it possible to offset the many disadvantages of conventional electrical machines, such as brushes and slip ring systems [3].

The BDFIGs offer an alternative for wind power generation due to their lower capital, operating costs and higher reliability compared to dual power induction generators. The stator of this machine comprises two sets of three-phase windings with a different number of poles, a power winding (PW) and a control winding (CW) [3].

To ensure the conversion of wind energy, several control strategies have been proposed in order to properly control the exchange of power between different elements of this system. Vector control, based on the classic PI controller is traditionally used for the control of the active and reactive powers of the BDFIG [4-6]. However, the main drawback of this controller is that its performance strongly depends on the parameters of the drive. Known for its robustness and simplicity of implementation, the Sliding Mode Control (SMC) has been widely used to control a large class of nonlinear systems [7-10].

This control law represents a drawback resided in the use of the sign function in the control law to ensure the transition from the phased approach to that of sliding. This gives rise to the chattering phenomenon, which consists of sudden and rapid variations in the control signal, which can excite the high frequencies of the process and damage it. Indeed, to remedy the drawback of this phenomenon, several works have been performed [11-15].

Artificial intelligence methods have been combined with sliding mode control-to-control non-linear systems with uncertainties and at least to eliminate the chattering phenomenon. Fuzzy logic control [16,17] is often used in complex systems to overcome the limitations of conventional mathematical tools. It nevertheless has limits, in particular on the accuracy of the information expressed in natural language, thus presenting a certain margin of instability. Fuzzy sliding mode controller (FSMC) [18] was designed to control the reactive and active powers of the BDFIG. The main drawback of FSMC is the lack of systematic methods for designing fuzzy and functional rule, Lyapunov methods [19]. Although this method reduces chattering, but the controller becomes continuous and the SMC characteristics, such as convergence, robustness, cannot be achieved and steady state errors may occur.

To overcome these drawbacks, the current trend is to integrate these tools into hybrid architectures to take advantage of the fuzzy logic and neural networks. The use of a fuzzy neural network offers the possibility of modeling a priori knowledge and linguistic decision rules obtained by experts in the field [20-25]. Various studies show that the ANFIS Neuro-fuzzy system, known as adaptive networks based on fuzzy inference, is able to quickly learn the behavior of a system with precision, and is even better than the other methods.

The NFSMC controller is proposed in this paper to regulate the active and reactive powers of a BDFIG.

2. MODELING OF THE BRUSHLESS DOUBLY FED INDUCTION GENERATOR

A BDFIG is depicted in Figure 1. The BDFIG dynamic equations in the reference d-q form can be written as follows [3]. The expressions for stators, rotor voltage and flux equations are given below.

2. 1. Stator Voltage Power SP

$$V_{sp}^{q} = R_{sp}I_{sp}^{q} + \frac{d\psi_{sp}^{q}}{dt} + \omega_p\psi_{sp}^{d}$$
$$V_{sp}^{d} = R_{sp}I_{sp}^{d} + \frac{d\psi_{sp}^{d}}{dt} - \omega_p\psi_{sp}^{q} \quad (1)$$

2. 2. Rotor Voltage

$$0 = R_rI_r^{q} + \frac{d\psi_r^{q}}{dt} + \omega_r\psi_r^{d}$$
$$0 = R_rI_r^{d} + \frac{d\psi_r^{d}}{dt} - \omega_r\psi_r^{q} \quad (2)$$

2. 3. Stator Voltage Control Power SC

$$V_{sc}^{q} = R_{sc}I_{sc}^{q} + \frac{d\psi_{sc}^{q}}{dt} + \omega_c\psi_{sc}^{d}$$
$$V_{sc}^{d} = R_{sc}I_{sc}^{d} + \frac{d\psi_{sc}^{d}}{dt} - \omega_c\psi_{sc}^{q} \quad (3)$$

2. 4. Stator Power Magnetic Flux

$$\psi_{sp}^{q} = L_{sp}I_{sp}^{q} + L_{mp}I_r^{q}$$
$$\psi_{sp}^{d} = L_{sp}I_{sp}^{d} + L_{mp}I_r^{d} \quad (4)$$

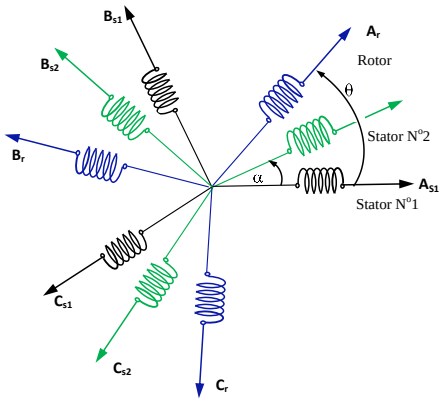

Figure 1. Configuration of a BDFIG

2. 5. Rotor Magnetic Flux

$$\begin{aligned}\psi_r^q &= L_r I_r^q + L_{mc} I_{sc}^q + L_{mp} I_{sp}^q \\ \psi_r^d &= L_r I_r^d + L_{mc} I_{sc}^d + L_{mp} I_{sp}^d \\ \psi_{sc}^q &= L_{sc} I_{sc}^q + L_{mc} I_r^q \\ \psi_{sc}^d &= L_{sc} I_{sc}^d + L_{mc} I_r^d\end{aligned} \tag{5}$$

The stator active and reactive power can be written according to the stator currents as:

$$\begin{aligned}P_{sp} &= \tfrac{3}{2}\left(V_{sp}^d I_{sp}^d + V_{sp}^q I_{sp}^q\right) \\ Q_{sp} &= \tfrac{3}{2}(V_{sp}^q I_{sp}^d - V_{sp}^d I_{sp}^q)\end{aligned} \tag{6}$$

The electromagnetic torque is given by:

$$T_{em} = \tfrac{3}{2}(P_p . L_{mp}(I_{sp}^q . I_r^d - I_{sp}^q . I_r^q) + P_c L_{mc}(I_{sc}^q . I_r^d - I_{sc}^d . I_r^q)) \tag{7}$$

3. VECTOR CONTROL STRATEGY OF BDFIG

The objective of the vector control (VC) of BDFIG is to obtain a decoupled control of the active and reactive powers as in DC machines [6]. The vector control of BDFIG consists of making:

$$\psi_{sp}^d = \psi_{sp} \qquad \psi_{sp}^q = 0 \tag{8}$$

The stator flux equation of the winding power becomes:

$$\begin{aligned}0 &= L_{sp} I_{sp}^q + L_{mp} I_r^q \\ \psi_{sp}^d &= L_{sp} I_{sp}^d + L_{mp} I_r^d\end{aligned} \tag{9}$$

By neglecting resistances of the stator phases, the stator voltage will be expressed by:

$$\begin{aligned}V_{sp}^d &= 0 \\ v_{sp}^q &= V_{sp} = \psi_{sp}^d . \omega_{sp}\end{aligned} \tag{10}$$

From Equation (10), Equation (6) becomes:

$$\begin{aligned}P_{sp} &= \tfrac{3}{2}\left(V_{sp}^q I_{sp}^q\right) \\ Q_{sp} &= \tfrac{3}{2}(V_{sp}^q I_{sp}^d)\end{aligned} \tag{11}$$

The rotor currents by:

$$\begin{aligned}I_{sp}^q &= \tfrac{-L_{mp}}{L_{sp}} I_r^q \\ I_{sp}^d &= \tfrac{\psi_{sp}^d - L_{mp} I_r^d}{L_{sp}}\end{aligned} \tag{12}$$

$$\begin{aligned}I_r^q &= \tfrac{\psi_r^q - L_{mp} . I_{sp}^q - L_{mc} I_{sc}^q}{L_r} \\ I_r^d &= \tfrac{\psi_r^d - L_{mp} . I_{sp}^d - L_{mc} I_{sc}^d}{L_r}\end{aligned} \tag{13}$$

We replace the expressions of the currents in Equation (12) we find:

$$\begin{aligned}I_{sp}^q \left(1 - \tfrac{L_{mp}^2}{L_{sp} L_r}\right) &= \tfrac{-L_{mp}}{L_{sp} L_r} \psi_r^q + \tfrac{-L_{mp} L_{mc}}{L_{sp} L_r} I_{sc}^q \\ I_{sp}^d \left(L_{sp} L_r - L_{mp}^2\right) &= L_r \psi_{sp}^d - L_{mp} \psi_r^d + L_{mp} L_{mc} I_{sc}^d\end{aligned} \tag{14}$$

After simplification, we obtain:

$$\begin{aligned}I_{sp}^q &= \tfrac{-L_{mp}}{L_{sp} . L_r - L_{mp}^2} \psi_r^q + \tfrac{L_{mp} . L_{mc}}{L_{sp} . L_r - L_{mp}^2} I_{sc}^q \\ I_{sp}^d &= \tfrac{L_r}{L_{sp} . L_r - L_{mp}^2} \psi_{sp}^d - \tfrac{L_{mp}}{L_{sp} . L_r - L_{mp}^2} \psi_r^d + \tfrac{L_{mp} . L_{mc}}{L_{sp} . L_r - L_{mp}^2} I_{sc}^d\end{aligned} \tag{15}$$

where:

$$\begin{aligned}&\delta_1 = \tfrac{L_{mp} L_{mc}}{L_{sp} L_r - L_{mp}^2}, \delta_2 = \tfrac{L_{mc} L_{sp}}{L_{sp} L_r - L_{mp}^2}, \delta_3 = L_{sc} - \tfrac{L_{mc}^2 L_{sp}}{L_{sp} L_r - L_{mp}^2} \\ &\delta_4 = \tfrac{L_{mp}}{L_{sp} L_r - L_{mp}^2}, \delta_5 = \tfrac{L_r}{L_{sp} L_r - L_{mp}^2}\end{aligned} \tag{16}$$

The stator active and reactive powers can be written according to the stator currents as:

$$\begin{aligned}P_{sp} &= \tfrac{3}{2} V_{sp}^q \left[-\delta_4 \psi_r^q + \delta_1 I_{sc}^q\right] \\ Q_{sp} &= \tfrac{3}{2} V_{sp}^q \left[\delta_5 \psi_{sp}^d - \delta_4 \psi_r^d + \delta_1 I_{sc}^d\right]\end{aligned} \tag{17}$$

We replace the expression of the current $\left(I_r^d, I_r^q\right)$ of Equation (13) in Equation (5), we obtain:

$$\begin{aligned}\psi_{sc}^q &= L_{sc} I_{sc}^q + L_{mc}\left(\tfrac{\psi_r^q - L_{mp} I_{sp}^q - L_{mc} I_{sc}^q}{L_r}\right) \\ \psi_{sc}^d &= L_{sc} I_{sc}^d + L_{mc}\left(\tfrac{\psi_r^d - L_{mp} I_{sp}^d - L_{mc} I_{sc}^d}{L_r}\right)\end{aligned} \tag{18}$$

We put the current expression $\left(I_{sp}^q, I_{sp}^d\right)$of Equation (15) in Equation (18), we obtain:

$$\begin{aligned}\psi_{sc}^q &= L_{sc} I_{sc}^q + \tfrac{L_{mc}}{L_r}\left(\psi_r^q - L_{mp}\left(\tfrac{-L_{mp}}{L_{sp} . L_r - L_{mp}^2} \psi_r^q + \tfrac{L_{mp} . L_{mc}}{L_{sp} . L_r - L_{mp}^2} I_{sc}^q\right) - L_{mc} . I_{sc}^q\right) \\ \psi_{sc}^d &= L_{sc} I_{sc}^d + \tfrac{L_{mc}}{L_r}\left(\psi_r^d - L_{mp}\left(\tfrac{L_r}{L_{sp} . L_r - L_{mp}^2} \psi_{sp}^d - \tfrac{L_{mp}}{L_{sp} . L_r - L_{mp}^2} \psi_r^d + \tfrac{L_{mp} . L_{mc}}{L_{sp} . L_r - L_{mp}^2} I_{sc}^d\right) - L_{mc} . I_{sc}^d\right)\end{aligned} \tag{19}$$

Finally:

$$\begin{aligned}\psi_{sc}^q &= \delta_3 I_{sc}^q + \delta_2 \psi_r^q \\ \psi_{sc}^d &= \delta_3 I_{sc}^d + \delta_2 \psi_r^d - \delta_1 \psi_{sp}^d\end{aligned} \tag{20}$$

We put the expression of the flux $\left(\psi_{sc}^q, \psi_{sc}^d\right)$ in Equation (3), we obtain the stator voltage as follows:

$$V_{sc}^q = R_{sc} I_{sc}^q + \tfrac{d}{dt}\left(\delta_3 I_{sc}^q + \delta_2 \psi_r^q\right) + \omega_c\left(\delta_3 I_{sc}^d + \delta_2 \psi_r^d - \delta_1 \psi_{sp}^d\right) \tag{21}$$

$$V_{sc}^{d} = R_{sc}I_{sc}^{d} + \frac{d}{dt}\left(\delta_3 I_{sc}^{d} + \delta_2\psi_r^{d} - \delta_1\psi_{sp}^{d}\right) - \omega_c\left(\delta_3 I_{sc}^{q} + \delta_2\psi_r^{q}\right)$$

Block diagram of the vextor control of BDFIG is shown in Figure 2.

4. SLIDING MODE CONTROL

Sliding mode control has been widely used in robust control approaches in many non-linear control method, the basic idea that if we can force a system to evolve towards an equilibrium point according to a dynamic chosen by the designer using the continuous control law.

The proposed sliding surface is used in this work [8]:

$$S(x) = (\frac{d}{dt} + \lambda)^{n-1} \times e \tag{22}$$

λ: is a positive coefficient,
$e = x_d - x$: is the error,
x_d: is the desired state,
n: is the system order.

4. 1. Switching Surface Let the monovariable dynamic system described by the following state equation [8]:

$$\dot{x} = f(x,t) + B(x,t).u(x,t) \tag{23}$$

where: $x \in R^n$ is the state variable, $u(x,t) \in R^n$ is the control vector, $B(x,t)$ are system parameter. The generalized SMC law is given as:

$$\begin{aligned} U &= U_n + U_{eq} \\ U_n &= K \times sign(s(x,t)) \end{aligned} \tag{24}$$

where, U is the control vector, U_{eq} is the equivalent control vector, *sign* is the signum function, K is the controller gain, s is the sliding surface. Figure 3 shows the sliding mode control block.

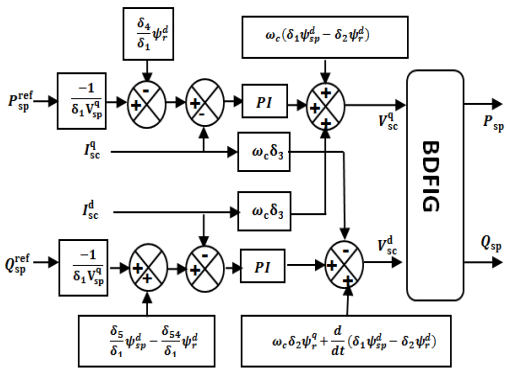

Figure 2. Block diagram of the vector control of BDFIG

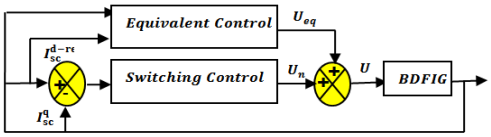

Figure 3. Sliding mode control block.

4. 2. Indirect Power Control with SMC of a BDFIG In this section, the sliding surfaces are designed according to the current references of the stator control. The objective of this design is to independently control the generated active and reactive powers.

4. 2. 1. Choice of the Sliding Surface Control Two sliding currents surfaces are used a first order is defined as:

$$\begin{aligned} S(I_{sc}^{q}) &= (I_{sc}^{q\_ref} - I_{sc}^{q}) \\ S(I_{sc}^{d}) &= (I_{sc}^{d\_ref} - I_{sc}^{d}) \end{aligned} \tag{25}$$

where $I_{sc}^{q\_ref}, I_{sc}^{d\_ref}$ are the expected currents of control power reference.

We have voltages in Equation (21), it can be used to extract the expressions of control current:

$$\begin{aligned} \dot{I}_{sc}^{q} &= \frac{1}{\delta_3}\left[V_{sc}^{q} - R_{sc}I_{sc}^{q} - \delta_2\dot{\psi}_r^{q} - \omega_c(\delta_3 I_{sc}^{d} + \delta_2\psi_r^{d} - \delta_1\psi_{sp}^{d})\right] \\ \dot{I}_{sc}^{d} &= \frac{1}{\delta_3}\left[V_{sc}^{d} - R_{sc}I_{sc}^{d} - \delta_2\dot{\psi}_r^{d} + \omega_c(\delta_3 I_{sc}^{q} + \delta_2\psi_r^{q})\right] \end{aligned} \tag{26}$$

5. CONDITIONS OF CONVERGENCE OF THIS CONTROL

To guarantee the convergence of the selected variables towards the references, the two sliding surfaces must be zero as follows:

$$\begin{aligned} S(I_{sc}^{q\_ref} - I_{sc}^{q}) = 0 \Rightarrow \frac{d}{dt}(I_{sc}^{q\_ref} - I_{sc}^{q}) = 0 \\ S(I_{sc}^{d\_ref} - I_{sc}^{d}) = 0 \Rightarrow \frac{d}{dt}(I_{sc}^{d\_ref} - I_{sc}^{d}) = 0 \end{aligned} \tag{27}$$

The sliding area of the current control can be defined as follows:

$$\begin{aligned} \dot{S}(I_{sc}^{q}) &= (\dot{I}_{sc}^{q\_ref} - \dot{I}_{sc}^{q}) \\ \dot{S}(I_{sc}^{d}) &= (\dot{I}_{sc}^{d\_ref} - \dot{I}_{sc}^{d}) \end{aligned} \tag{28}$$

$$\begin{aligned} \dot{S}(I_{sc}^{q}) &= \dot{I}_{sc}^{q\_ref} - \frac{1}{\delta_3}\left[V_{sc}^{q} - R_{sc}I_{sc}^{q} - \delta_2\dot{\psi}_r^{q} - \omega_c(\delta_3 I_{sc}^{d} + \delta_2\psi_r^{d} - \delta_1\psi_{sp}^{d})\right] \\ \dot{S}(I_{sc}^{d}) &= \dot{I}_{sc}^{d\_ref} - \frac{1}{\delta_3}\left[V_{sc}^{d} - R_{sc}I_{sc}^{d} - \delta_2\dot{\psi}_r^{d} + \omega_c(\delta_3 I_{sc}^{q} + \delta_2\psi_r^{q})\right] \end{aligned} \tag{29}$$

5. 1. Control Law The satisfactions of the control voltage and sign function are presented in the following:

$$\begin{aligned} V_{sc}^{d} &= V_{sc}^{d\_eq} + V_{sc}^{d\_att} \\ V_{sc}^{d_{att}} &= K_d \times sign\big(s(x,t)\big) \\ V_{sc}^{q} &= V_{sc}^{q_{eq}} + V_{sc}^{q_{att}} \\ V_{sc}^{q\_att} &= K_q \times sign(s(x,t)) \end{aligned} \tag{30}$$

with

V_{sc}^{d}, V_{sc}^{q} : Control vectors relation.

$V_{sc}^{d\_eq}, V_{sc}^{q\_eq}$: Equivalent control vectors relation.

$V_{sc}^{d\_att}, V_{sc}^{q\_att}$: Switching control.

K_d, K_q : Positive constant.

From Equation (29), the voltage equivalent control is given by:

$$\begin{aligned} &\dot{S}(I_{sc}^{q}) = 0 \;\Rightarrow\; V_{sc}^{q_{eq}} = \delta_3 \dot{I}_{sc}^{q_{ref}} + R_{sc} I_{sc}^{q} + \\ &\delta_2 \dot{\psi}_r^{q} + \omega_c\big(\delta_3 I_{sc}^{d} + \delta_2 \psi_r^{d} - \delta_1 \psi_{sp}^{d}\big) \\ &\dot{S}(I_{sc}^{d}) = 0 \;\Rightarrow\; V_{sc}^{d\_eq} = \delta_3 \dot{I}_{sc}^{d\_ref} + R_{sc} I_{sc}^{d} + \\ &\delta_2 \dot{\psi}_r^{q} - \omega_c(\delta_3 I_{sc}^{q} + \delta_2 \psi_r^{q}) \end{aligned} \tag{31}$$

The global BDFIG sliding-mode control are depicted in Figure 4.

6. NEURO-FUZZY ARCHITECTURE

Hybrid systems that combine fuzzy logic, neural networks, genetic algorithms, and expert systems have proven their effectiveness in a variety of real-world problems and in industry. Each intelligent technique has specific properties. Each technique is suitable for solving certain particular problems. In fact, neural networks are used for the recognition of models. However, they are unable to explain how they reach their decisions. Fuzzy logic systems can reason with imprecise information and explain their decisions but cannot, however, automatically acquire the rules they used to make those decisions. These limits have been a reason behind the creation of intelligent hybrid systems where; two or more techniques are combined to overcome the limitations of one technique [23].

Adaptive neural based on fuzzy inference system ANFIS uses feedback learning to determine the input parameters and parameters used. Each step of the iterative learning algorithm has two parts. In the first part, the input models are propagated and the parameters of the parameters are calculated using the iterative minimal square method algorithm, while the parameters of the premises are considered fixed. In the second part, the input models are propagated again, and at each iteration, the back propagation learning algorithms are used to modify the parameters of the premises, while the consequences remain fixed.

6. 1. Adaptive Neuro-fuzzy Sliding Mode Control Inference System A typical diagram of a ANFIS is shown in Figure 5, in which a circle indicates a fixed node on one hand, and a square implies an adaptation node on the other hand [13]. In addition, x, y stand for two inputs and one output, Sugeno fuzzy is often used in various fuzzy inference models for the following reasons: high interpretability, increased efficiency and adaptation techniques where the number of epochs is set to 40 and error tolerance of 10^{-6} [23].

The direct current error *(e, de)* is two inputs of ANFIS control in our system defined as:

$$\begin{aligned} e &= I_{sc}^{q_{ref}} - I_{sc}^{q} \rightarrow de = I_{sc}^{q_{ref}} - I_{sc}^{q} \\ e &= I_{sc}^{d\_ref} - I_{sc}^{d} \rightarrow de = I_{sc}^{d\_ref} - I_{sc}^{d} \end{aligned} \tag{32}$$

where, (*e*,*de*) is the first order Sugeno case fuzzy inference employed by ANFIS, and the function fuzzy rule is:

If $e$is $A_i$and $de$is $B_i$then $y=f(e,de)$. Corresponding to the architecture of ANFIS which consists of five layers. The steps of ANFIS structure are:

Layer 1: Each corresponding node during this layer creates the membership range for the input vectors A_i, $i=1....7$.

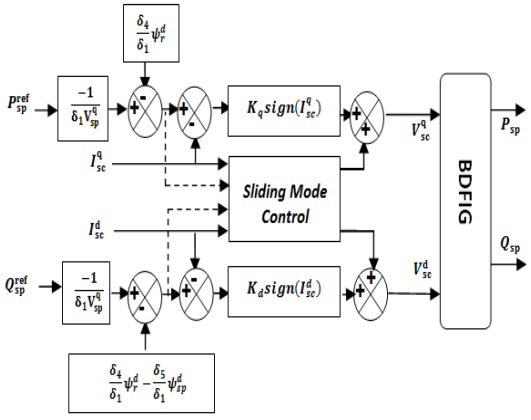

Figure 4. Block diagram of BDFIG sliding mode control

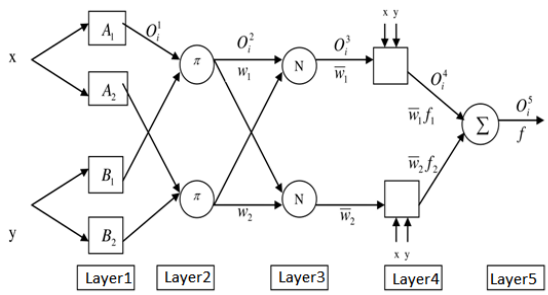

Figure 5. ANFIS architecture

Layer 2: The node generates the crossing by multiplying all the incoming signals:$O_i^2 = w_i = \mu_{A_i}(x)\mu_{B_i}(y)$, for $i = 1,\ldots 49$.

Average nodes (Layer 3): Divided by the sum of all other entries.

$$O_i^3 = \overline{w_i} = \frac{w}{\sum_{i=1}^{49} w_i} \quad (33)$$

Consequent nodes (Layer 4): Compute the contribution of the i-th rule in the output with the following node function.

$$O_i^4 = \overline{w_i} y_i = \overline{w_i}(p_i e + q_i de + r_i)$$

where, $\overline{w_i}$ is the output of layer 3, and *(pi, qi, ri)* are the parameter set of the '*i-th'* node.

Output node (Layer 5): The neuron of layer 5 is a fixed neuron, at a given input; it delivers the network response given by:

$$O_i^5 = \sum_{i=1}^{49} \overline{w_i} f_i = \frac{\sum_{i=1}^{49} w_i f_i}{\sum_{i=1}^{49} w_i} \quad (34)$$

6. 2. Description of the Control System

Figure 6 shows the proposed Neuro-Fuzzy-Sliding Mode Control for controlling the active and reactive powers of the BDFIG. NFSMC controller replaces the switching control of SMC, the first input is the error of the current and the second input is the derivative of the error. Figure 6 shows the neuro-fuzzy sliding mode control

7. SIMULATION RESULTS

Different power control methods have been studied and modeled with Matlab / Simulink software under the same test conditions powered by an PWM inverter. Simulations were applied to the 2.5 kW BDFIG system incorporating the NFSMC compared with the SMC and PI control. The parameters of the BDFIG system are illustrated and appended to Table 1 where the speed is fixed at 73 rad /s.

Figure 7 presents the NFSMC test with training and cheking of reactive and active power reference error data sets after 40 epochs to guarantee good performance of results.

Figures 8 and 9 show the active and reactive powers produced by BDFIG with the different control strategies,VC, SMC and NFSMC. In these figures, we

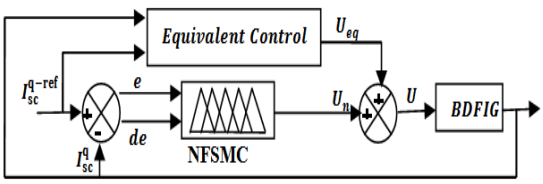

Figure 6. Neuro-Fuzzy-Sliding Mode Control

TABLE 1. BDFIG parameters

Power Winding (PW)	Control Winding (CW)	Rotor
$R_{sp} = 1.732(\Omega)$	$R_{sc} = 1.079(\Omega)$	$R_r = 0.473(\Omega)$
$L_{sp} = 714.8(mH)$	$L_{sc} = 121.7(mH)$	$L_r = 132.6(mH)$
$L_{mp} = 242.1(mH)$	$L_{mc} = 59.8(mH)$	
$p_p = 3;\quad P_n = 2.5KW$	$p_c = 1$	

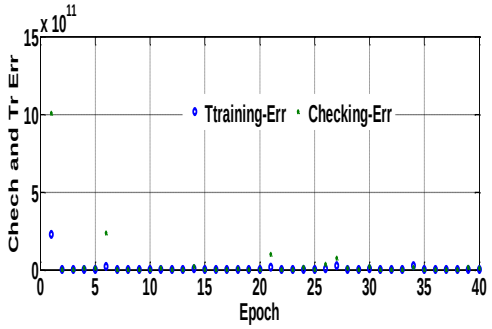

Figure 7. NF-SMC training and checking error of active power

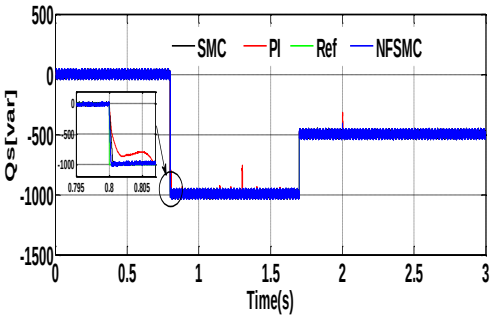

Figure 8. Reactive power response

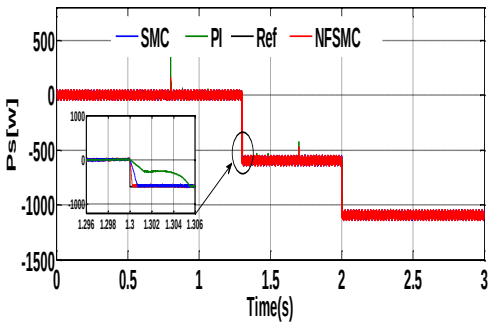

Figure 9. Active power response under VC, SMC and NFSMC strategies

can notice that the ripple is not the same for the three techniques, it is clear that the VC suffers from two problems: stabilizing error and high ripples in the active power. On the other hand, the NFSMC offers an almost

perfect behavior in terms of performance and good follow-up compared to the PI and SMC.

Figure 10 shows the stator current on phase A, with sinusoidal shapes for the three strategies. We can observe that the current ripple also has a significant reduction of the NFSMC controller compared to the other controller.

7. 1. Simulation Results with Parametric Uncertainty To study the influence of the electrical parameter variation on the behavior of the BDFIG, we also simulated the system for a +100% of the nominal stator resistance at time t = 2.5s.

Figures 11 and 12 illustrate the evolution of the powers. We note from this result that the scheme (PI) has a slight variation due to the variations of stator resistance. The proposed NFSMC method is robust against parameter variations and allows a fast and suitable dynamic response.

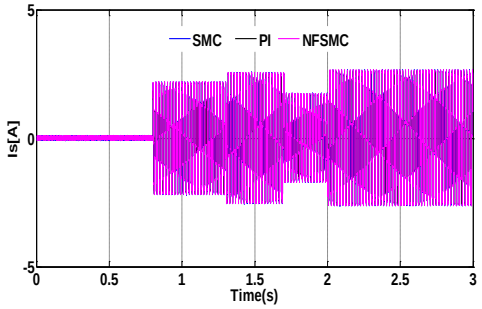

Figure 10. Stator current I_{sa} of three approaches

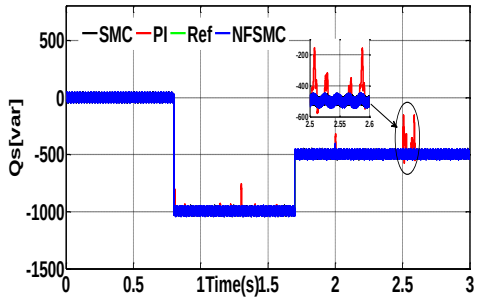

Figure 11. Reactive power under stator resistance variation

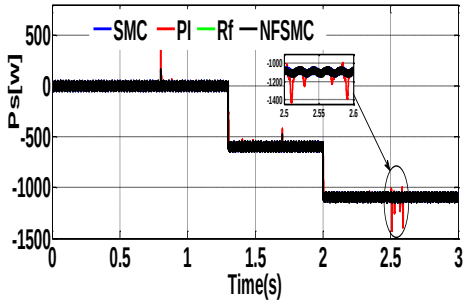

Figure 12. Active power under stator resistance variation

Table 2 presents the quantitative analysis of the three approaches. The comparison implicates that the proposed NFSMC gives less chattering with a seamless transient response.

TABLE 2. Performances comparison of the three controllers

Approach	VC	SMC	NFSMC
Robustness to parameters mismatch	High	Low	Low
Chattering	Medium chattering	Considerable chattering	Small chattering
Transient performance of the active power	Relatively fast with medium settling time	Relatively fast with low settling time	Fast with low settling time
Rising time of the active power	0.16 s	0.12S	0.01 s
Transient performance of the reactive power	Relatively fast with medium settling time	Relatively fast with low settling time	Fast with low settling time
Rising time of the reactive power	0.18 s	0.14 s	0.016 s
Implementation Complexity	High	Low	Low

8. CONCLUSION

In this paper, Neuro-Fuzzy Sliding Mode Control NFSMC for BDFIG has been presented. The suggested control has been compared with the classical vector control based on PI controller and sliding mode control. Simulation results demonstrate that the powers' ripples is lower in NFSMC compared with the other controls. The efficiency of the proposed NFSMC has been validated by simulation tests carried out with a 2.5 KW BDFIG system. Moreover, to validate the influence of BDFIG parameter variations on the performances of the proposed NFSMC, sensitivity of the stator resistance parameter has been tested for the three schemes for +100% variations in stator resistance. It has been shown that the proposed approach is robust and capable to reject the influences of uncertainty in system parameters.

9. REFERENCES

1. Protsenko, K. and Xu, D., "Modeling and control of brushless doubly-fed induction generators in wind energy applications". ***IEEE Transactions on Power Electronics***, Vol.23, No3, (2008), 1191–1197.
2. Tazil, M., Kumar, V., and Kong, S. "Three-Phase doubly fed induction generator: An over view", ***IET Electric Power Application***, (2009), 75–89.

3. Jing, C., Xuefan, W., Tantan, Z., Zhenping, L., Ming, K. and,Pengcheng, N., "Application of Brushless Doubly-Fed Machine System Hydropower Generation". 2nd International Conference on Electrical Machines and Systems (ICEMS). IEEE, (2019), 1-4.
4. Sheng, H., and Guorong Z., "A Vector Control Strategy of Grid-Connected Brushless Doubly Fed Induction Generator Based on the Vector Control of Doubly Fed Induction Generator", 2016 IEEE Applied Power Electronics Conference and Exposition (APEC).
5. Chen, J. F., Zhang, W., Chen, B. J., and Ma, Y. L., "Improved vector control of brushless doubly fed induction generator under unbalanced grid conditions for offshore wind power generation", ***IEEE Trans. Energy Conv***. Vol.31, (2016), 293-302.
6. Shiyi, S. , Ehsan, A. , Farhad, B. , and Richard, M., "Stator-Flux-Oriented Vector Control for Brushless Doubly Fed Induction Generator", ***IEEE Transactions on Industrial Electronics,*** Vol. 56,(2009),4220 – 4228.
7. Mahboub, M. A, and Drid, S. "Sliding mode control of a Brushless doubly fed induction generator", Proceedings of IEEE (ICSC) the 3rd Intel Conference on Systems and Control, Algeria, 2013.
8. Mazouz, F., Belkacem, S., Colak, I., and Drid, S., "Direct Power Control of DFIG by Sliding Mode Control and Space Vector Modulation", 7th International conference on system and control, IEEE (ICSC), Valencia – Spain, October, (2018),24-30.
9. Daoud, A., and Derbel, N., "Direct Power Control of DFIG Using Sliding Mode Control Approach",In Modeling, Identification and Control Methods in Renewable Energy Systems Springer, Singapore, (2019), 193-204.
10. Douadi, T., Y. Harbouche, R. Abdessemed, and I. Bakhti, "Improvement performances of active and reactive power control applied to DFIG for variable speed wind turbine using sliding mode control and FOC*." **International Journal of Engineering- Transactions A: Basics***, Vol. 31, No.10, (2018), 1689-1697.
11. Yang, J., Jian, Y., Weiy, T., Guanguan, Z., Yao, S., Sul, A., and Frede, B., "Sensorless Control of Brushless Doubly Fed Induction Machine Using a Control Winding Current MRAS Observer." ***IEEE Transactions on Industrial Electronics,*** Vol. 66, No.1, (2019), 728-738.
12. Juan, I., T, Paul, F.P., Marcelo, G.C., and José, A.,"A Dual-Stator Winding Induction Generator Based Wind-Turbine Controlled via Super-Twisting Sliding Mode". ***Energies***, Vol.12, (2019, 223-230.
13. Roberto, C., Pena, R. , Wheeler, and Clare, P.,"Control of a wind generation system based on a Brushless Doubly-Fed Induction Generator fed by a matrix converter", ***Electric Power Systems Research,*** Vol.103, (2013), 49–60.
14. Maryam, M., Rasool, K., and Mohammad, R.A. "Model-based predictive direct power control of brushless doubly fed reluctance generator for wind power "***Alexandria Engineering Journal***, Vol. 55, (2016), 2497-2507.
15. Mahyar, G., Ashknaz, O., Sajjad, T., Hashem, O., and Richard A.M., "An analytical study for low voltage ride through of the brushless doubly-fed induction generator during asymmetrical voltage dips" ***Renewable Energy***, Vol. 115, 2018, 64-75.
16. Belkacem, S., Naceri, F., and Abdessemed, R., "Reduction of torque ripple in DTC for induction motor using input-output feedback linearization", ***Turkish Journal of Electrical Engineering & Computer Sciences***, Vol**.** 20, No. 3, (2012).1123-1130.
17. Youb, L., Belkacem**,** S, Naceri, F, Cernat, M, and Guasch, L. P, "*Design of an Adaptive Fuzzy Control System for Dual Star Induction Motor Drives*", ***Advances in Electrical and Computer Engineering***, Vol. 18, No. 3, (2018).
18. Larbi, D. and Loukianov, A.G. , "Neural Sliding Mode Control of a DFIG Based Wind Turbine with Measurement Delay", ***International Federation of Accountants*** ,Vol. 51, (2018), 456-461.
19. Abdelbasset, M., Drid, S., Sid, M.A., and Ridha, C. "Robust direct power control based on the Lyapunov theory of a grid-connected brushless doubly fed induction generator". ***Frontiers in Energy***, Vol.10, (2016), 298-307.
20. Tiwari, N. K, Parveen, S., Bhupendra, K. S., Subodh, R, and Krishna, K. S."Estimation of Tunnel Desilted Sediment Removal Efficiency by ANFIS. ***Iranian Journal of Science and Technology, Transactions of Civil Engineering***, (2019), 1-16.
21. Asar, M. F., Elawady, W M., and Sarhan, A M. "ANFIS-based an adaptive continuous sliding-mode controller for robot manipulators in operational space". ***Multibody System Dynamics***, (2019), 10-21.
22. Sana, B., and Anis, S., "Adaptive Neuro-Fuzzy Sliding Mode Controller", ***International Journal of System Dynamics Applications***, Vol. 7, (2018).
23. Ifte, K.A., Uddin, M.N. , and Marsadek, M. "ANFIS Based Neuro-Fuzzy Control of DFIG for Wind Power Generation in Standalone Mode", *2019 IEEE* International Electric Machines & Drives Conference (IEMDC).
24. Ibrahim, F.B., Ahmed, A., Ahmed, T., and Ahmed, L., "Robust neuro-fuzzy sliding mode control with extended state observer for an electric drive system". **E*nergy***, Vol. 169, (2018).
25. Mazouz, F., Belkacem, S**.**, Drid, S., Chrifi, A.L. and Colak I., "*Fuzzy Sliding Mode Control of DFIG applied to the WECS*". Proceedings of the 8th International Conference on Systems and Control, Marrakech, Morocco, October 23-25, 2019.

Neuro-fuzzy Sliding Mode Controller Based on a Brushless Doubly Fed Induction Generator

L. Ouada[a], S. Benaggoune[a], S. Belkacem[b]

[a] *Faculty of Technology, LSTE Laboratory, University of Mostefa Ben Boulaïd Batna 2, Algeria*
[b] *LEB Research Laboratory, Electrical Engineering Department, University of Mostefa Ben Boulaïd Batna 2, Algeria*

P A P E R I N F O

Paper history:
Received 30 June 2019
Received in revised form 07 January 2020
Accepted 16 January 2020

Keywords:
Brushless Doubly Fed Induction Generator
Neuro-fuzzy Sliding Mode Control
Parameters Uncertainly
Sliding Mode Control
Vector Control

چکیده

ترکیبی از شبکه‌های عصبی و کنترل‌کننده‌های فازی به عنوان کارآمدترین روش برای تقریب توابع مختلف در نظر گرفته شده است و نشان‌دهنده توانایی آنها در کنترل سیستم‌های دینامیکی غیرخطی است. در این مقاله یک استراتژی کنترل ترکیبی به نام کنترل حالت کشویی Neuro-Fuzzy (NFSMC) مبتنی بر ژنراتور القایی تغذیه شده Brushless Dushly (BDFIG) ارائه شده است. این جایگزین سطح کشویی کنترل می شود تا پدیده chattering ناشی از عملکرد کنترل ناپیوسته را حذف کند. این تکنیک ویژگی‌های جذابی مانند مقاومت به تغییرات پارامتر را ارائه می‌دهد. نتایج شبیه‌سازی ۲.۵ KW BDFIG برای تأیید اثربخشی و استحکام رویکرد پیشنهادی در حضور عدم قطعیت در رابطه با کنترل بردار (VC) و کنترل حالت کشویی (SMC) ارائه شده است. ما خصوصیات استاتیک و دینامیکی سه روش کنترل را تحت شرایط عملیاتی یکسان و در همان پیکربندی شبیه‌سازی مقایسه می‌کنیم. طرح‌های کنترل‌کننده پیشنهادی (NFSMC) در کاهش موج قدرت‌های فعال و واکنشی مؤثر هستند، به طور مؤثر سرکوب حالت‌های کشویی و اثرات عدم قطعیت‌های پارامتری بر عملکرد سیستم مؤثر نیستند.

***doi**: 10.5829/ije.2020.33.02b.09*